Environmental Science & Technology

pubs.acs.org/est

Article

Ecotoxico Linking of Phthalates and Flame-Retardant Combustion Byproducts with Coral Solar Bleaching

Ali Ranjbar Jafarabadi, Sakineh Mashjoor, Alireza Riyahi Bakhtiari,* and Tiziana Cappello

Cite This: https://doi.org/10.1021/acs.est.0c08730

Read Online

ACCESS | Metrics & More | Article Recommendations | Supporting Information

ABSTRACT: Persian Gulf coral reefs are unique biota communities in the global sunbelts in being able to survive in multiple stressful fields during summertime (>36 °C). Despite the high-growth emerging health-hazard microplastic additive type of contaminants, its biological interactions with coral−algal symbiosis and/or its synergistic effects linked to solar-bleaching events remain unknown. This study investigated the bioaccumulation patterns of polybrominated diphenyl ether (PBDE) and phthalate ester (PAE) pollutants in six genera of living/bleached corals in Larak Island, Persian Gulf, and their ambient abiotic matrixes. Results showed that the levels of $\sum_{18}$PBDEs and $\sum_{13}$PAEs in abiotic matrixes followed the order of SPMs > surface sediments > seawater, and the cnidarian POP-uptake patterns (soft corals > hard corals) were as follows: coral mucus (138.49 ± 59.98 and 71.57 ± 47.39 ng g^{-1} dw) > zooxanthellae (82.05 ± 28.27 and 20.14 ± 12.65 ng g^{-1} dw) ≥ coral tissue (66.26 ± 21.42 and 34.97 ± 26.10 ng g^{-1} dw) > bleached corals (45.19 ± 8.73 and 13.83 ± 7.05 ng g^{-1} dw) > coral skeleton (35.66 ± 9.58 and 6.47 ± 6.47 ng g^{-1} dw, respectively). Overall, findings suggest that mucus checking is a key/facile diagnostic approach for fast detection of POP bioaccumulation (PB) in tropical corals. Although studied corals exhibited no consensus concerning hazardous levels of PB (log BSAF < 3.7), our bleaching evidence showed soft corals as the ultimate "summer winners" due to their flexibility/recovering ability.

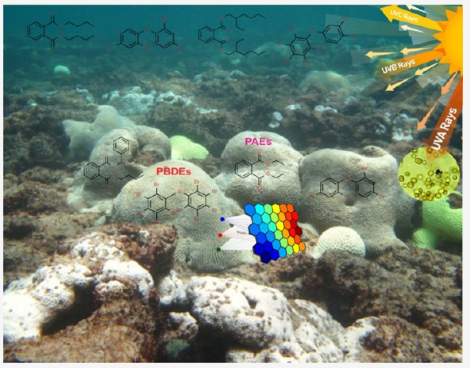

1. INTRODUCTION

Globally, corals are recognized as effective bioindicators for evaluating the water quality status because of their ecological significance and high productivity/biodiversity and being key sessile organisms.[1] Coral reefs are unique albeit fragile ecosystems that host more than a quarter of all marine life and are subjected to threats of anthropogenic stressors (e.g., chemical contamination) at universal and local scales.[2]

In coral−algal symbiosis relationships, *Symbiodinium* (zooxanthellae) is used as a diagnostic tool for environmental stress in crucial ecosystems: once damaged, symbiotic disruption occurs, resulting in symbiont-depleted corals (bleaching) and consequent changes in the ratio of zooxanthellae to coral biomass.[3] Furthermore, photodamage in coral tissues and zooxanthellae due to exposure to elevated light and ultraviolet irradiance, in combination with high temperatures, is a major factor in eliciting solar bleaching.[4] Nonetheless, there is no evidence that the interaction between the solar-bleaching process and organic contaminants in leachates from coastal landfills and seafills is synergistic. Rather, it appears that these factors showed simple additive effects, but clearly, more research is needed. More importantly, it is confirmed that cnidarian mucus has a vital role in coral health since it is primarily involved in the cleansing mechanisms against pollutants by an intense mucus production in corals.[1,5] However, environmental pollution studies on scleractinian mucus are still scarce.

One of the global environmental threats associated with the combustion of organic products such as organohalogen flame retardants is the potential for emerging toxic chemicals in terms of waste to energy, particularly in the warmer conditions of marine environments, which may dictate an improved UV photolysis system for reformation and/or degradation of hazardous pollutants.[6,7] The maxima phototoxicity and absorption of persistent organic pollutants (POPs) fall within the range of ultraviolet radiation (UVR: UVA (320−400 nm) > UVB (280−320 nm)), which results in the formation of reactive oxygen species (ROS) and/or transformation of POPs into more toxic intermediate photoproducts in coral reefs.[8−103]

Bioaccumulation of gaseous emissions from co-combustion of sewage sludge products or other different combustion routes and photolytic degradation/oxidation of defined organic pollutants including synthetic brominated flame retardants (BFRs), polychlorinated dibenzo-p-dioxin and dibenzofuran (PCDD/F), petroleum hydrocarbons, phenanthrene, and associated plastic contaminants such as phthalate esters

Received: December 30, 2020
Revised: March 26, 2021
Accepted: April 6, 2021

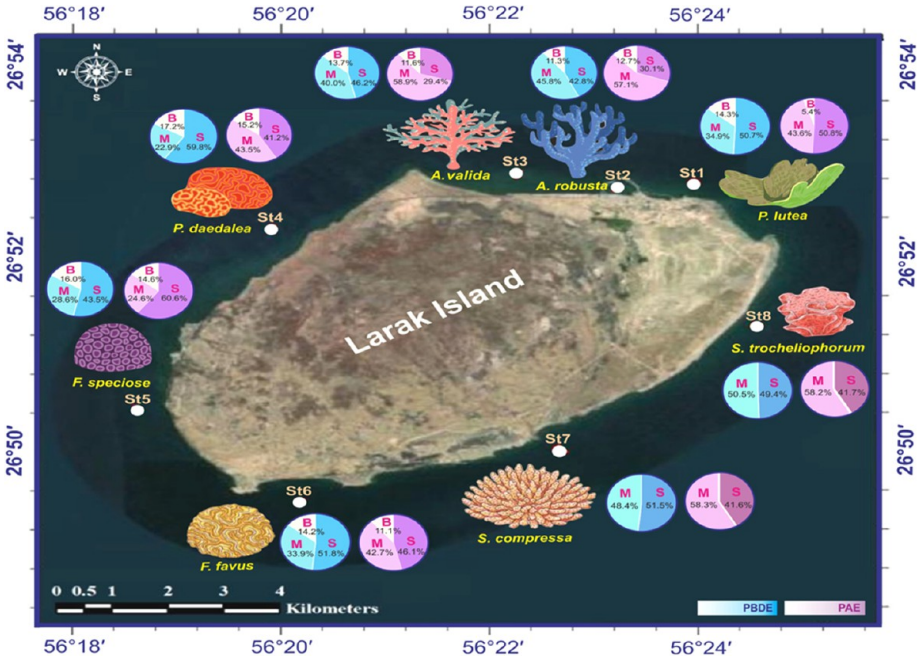

Figure 1. Spatial species-specific distribution of corals in the eight sampling sites of Larak Island (Persian Gulf, Iran). Pie charts refer to the occurrence of $\sum_{17}$PBDEs and $\sum_{13}$PAEs for stressed corals (S), bleached corals (B), and mucus of corals (M) in this in situ study.

(PAEs) in phytoplanktons and *de novo* transfer to corals may have contributed to degradation of coral reef communities and coral bleaching thresholds.[8−13] Polybrominated diphenyl ethers (PBDEs) are a class of BFRs consisting of 209 congeners,[6] which are persistent in the environment, including coral reef ecosystems. However, their biochallenges combined with other POPs such as PAEs (most used for the synthesis of poly(vinyl chloride) (PVC), color, glue, and styrene materials)[14] to coral bleaching susceptibility are not reported yet. Besides, there is considerable evidence that coral reef systems are highly affected by plastic (microplastic) debris, which contains organic elements of plastic materials such as PBDEs and PAEs, that could be accidentally captured by corals like plankton uptake, subsequently affecting coral health.[5,15] At the same time, plastic wastes are not well managed and could enter the marine environment (nearly 269 000 MT of plastics enters the oceans worldwide) via industrial activities or by the degradation of float macrodebris, impact the ecosystem functioning, and eventually accumulate in biota.[16,17] Both PBDEs and PAEs are emerging environmental contaminants due to their hydrophobicity and aquatrophic toxicity.[13,18,19] However, there is little information on their potential health risk, long-range airborne transport, leaching, discharge, aquasinking, biomagnification, and marine trophic transfer.[13,18,20−22] Herein, we would like to evaluate what direct/indirect items are issued upon receipt in coral reefs of even low levels (ng L^{-1} to μg L^{-1}) of these chemicals.

Over the last decade, the intensive anthropogenic intervention mainly due to Iranian oil/gas companies has been augmenting exponentially, leading to damage and shifts in the structure of the Persian Gulf coral reef communities.[23] In addition, extreme summer marine heatwaves (MHWs) can have devastating impacts on fragile reefs of the Persian Gulf, considered to be the hottest place on earth with the highest recorded bleaching thresholds in the world.[24] In 2015, the United States National Oceanic and Atmospheric Administration (NOAA) declared a major mass bleaching event as the "3rd global coral bleaching event".[25] The Persian Gulf was no exception, and the Larak Island (with the greatest taxon diversity including 44.67% of scleractinian fauna),[26] located in the central region of the Strait of Hormuz, was one of the most affected areas due to thermocline variability and MHWs from the Gulf of Oman. Hence, this area was herein chosen as the case study region for an eco-devo perspective[27] and coral co-poisoning with UVR, sea-surface temperature (SST) anomalies, and plastic additive (e.g., PBDEs and PAEs) contaminations, which can change the toxicokinetics end points referring to the summer coral bleaching crisis. Notably, the potential adverse effects of these natural/anthropogenic coral exposures and their contribution to the coral taxonomic response to bleaching susceptibility remain unknown. Herein, using the clustering self-organizing map (SOM), a type of artificial neural network (ANN) model, and network analysis (NA), the relationship between emission/bioaccumulation of PBDE and PAE congeners in abiotic matrixes of Larak Island and their partitioning in biocomponents of corals were deeply evaluated during the 2015 Persian Gulf solar-bleaching event.

2. MATERIALS AND METHODS

2.1. Satellite Radiation Products. For the wide monitoring of natural/seasonal environmental variables about coral bleaching such as the sea-surface temperature (SST) range, UVA, and solar irradiance throughout the Persian Gulf, including Larak Island, we employed the MODIS-Aqua data products of Level 3 to map daily and monthly SST thermal infrared (IR) data at 4−9 km resolution. At these sites, MODIS L3, 9 km, 11 μm, monthly daytime SST products for July as the hottest month in 2015 were obtained from http://oceancolor.gsfc.nasa.gov and, for worldwide analysis, the UV/solar radiation products in the second week of July (7/15/2015) were obtained from http://neo.sci.gsfc.nasa.gov (from NASA OBPG: Ocean Biology Processing Group (OBPG) at NASA's Goddard Space Flight Center). Graphs were visualized using NASA's Applied Remote Sensing Training Program,

https://doi.org/10.1021/acs.est.0c08730
Environ. Sci. Technol. XXXX, XXX, XXX−XXX

Panoply-4.6.1 (2016) (https://www.giss.nasa.gov/tools/panoply). Additional details on the UV index (UVI) data analysis[28,29] are provided in the Supporting Information (SI).

2.2. Coral Propagation and Field Data Collection. A comprehensive sampling was carried out in July 2015 (summer season) at various sites around fringing coral reefs of Larak Island (26°51′12″N 56°21′20″E), Persian Gulf, Iran. Fifty coral samples including 30 hermatypic (hard corals/reef-building) and 20 ahermatypic (soft corals/non-reef-building) coral samples from onshore sites were collected by divers utilizing a hammer and chisel. Reef-building corals included *Acropora robusta*, *Acropora valida*, *Platygyra daedalea*, *Favia favus*, *Favia speciosa*, *Porites lutea*, while non-reef-building ones were *Sinularia compressa* and *Sarcophyton trocheliophorum* (Figure 1). Their sizes were from fairly 7 cm × 7 cm to 14 cm × 12 cm. Coral samples were placed on preheated (500 °C) aluminum foils, held on ice when in the field, and then frozen within 6 h and afterward stored at −20 °C until analysis.

Seawater (SW; 0−40 cm, n = 40, 4 L of each sample) and surface sediment (SS; 0−5 cm, n = 40, 1 ± 0.2 kg of each sample) samples were collected with precleaned 4 L brown glass bottles and a Van Veen grab sampler and stainless steel containers. Samples were stored at −20 °C prior to further analysis. All seawater samples were filtered through 0.45 mm organic membrane filters to remove sand and debris from seawater samples.[31] To investigate the physicochemical parameters of water, we conducted the gold standard for the examination of water.[31] The water quality indexes (WQIs) included pH, dissolved oxygen (DO), biological oxygen demand (BOD), total organic carbon (TOC), nitrate (NO_3^{-1}), phosphate (PO_4^{-3}), and turbidity.

2.3. Analytical Process. The approach of Zhang et al.[32] was used to prepare the sediment samples for PBDEs. Briefly, this approach comprises Soxhlet extraction with a mixture of acetone and hexane (1:1), purification with a silica (neutral and sulfuric) SPE cartridge, and elution with a hexane:dichloromethane mixture (1:1, V/V). For SW samples, the method of Wang et al.[33] was used for PBDEs. The filtered samples were passed through the preconditioned SPE (LC-C18) cartridges. Then, they were eluted with methanol, dichloromethane, and n-hexane, and eventually, the resulted extracts were concentrated and purified with neutral silica based on the method of Ju et al.[34] and Saliu et al.[35] Agilent 7890A/5975A GC/MS equipped with a DB-5 MS UI capillary column was used for PAE analysis, while Shimadzu 2010 GC/MS equipped with a DB-XLB capillary column was applied for PBDE analysis. Compound identification was based on the m/z ratio of the selected ions and the comparison with the chromatograms of the standard mixture (purchased from AccuStandard, New Haven, CT). More details are provided in the Supporting Material.

To extract lipids from coral samples, the method of Folch et al.[36] was used. In this regard, coral tissues were segregated from the coral skeleton, applying a Waterpik with 1 L synthetic seawater. Then, using settlement and filtering (0.7 μm, GF/F filter, Whatman, England), coral tissues were separated from seawater. The tissue moisture content was calculated based on the difference in the tissue weight before and after freeze-drying. Coral mucus was in the filtrate, and coral samples were extracted by solid-phase microextraction (SPME) (a microwave-assisted solubilization of coral tissues in acetone).[35]

Instrumental analysis, identification, and quantification of PBDEs and PAEs were performed using a gas chromatograph coupled with a mass spectrometer (Varian CP-3800−Varian 320). In total, 18 PBDE congeners, namely, BDE17, BDE28, BDE42, BDE47, BDE49, BDE51, BDE66, BDE74, BDE85, BDE99, BDE100, BDE138, BDE153, BDE154, BDE183, BDE190, BDE191, and BDE209, and also 13 PAEs including DMP, DEP, DIBP, BBP, DNHP, DBP, DCHP, DEHP, DPP, DnBP, DnOP, DIDP, and DHP, were identified. More detailed information is presented elsewhere.[35]

2.4. Symbiodinium Isolation and Processing. Symbiotic algae were isolated from Larak Island corals, and their population density per unit area of the coral tissue was analyzed based on the method of Jafarabadi et al.[37] Then, chlorophyll-a (Chl-a) and -c (Chl-C_2) contents in symbiodinium and the ratio of Chl-a/Chl-C_2 (R1) were determined.[37]

2.5. Bioaccumulation Factor. In this study, the biota-sediment accumulation factor (BSAF) and bioconcentration factor (BCF) of detected PBDE and PAE organic compounds were calculated in the whole coral tissues (dry weight, dw) of each species to those dissolved in seawater (BCF, eq 1) and to those measured in the sediment (BAF, eq 2).[38,39] To normalize the coral lipid contents and their organic carbon in the bioaccumulation factor, eq 3 was used.

$$\mathrm{BCF} = \text{tissue } (\mathrm{ng\,g^{-1}dw})/\text{seawater } (\mathrm{ng\,L^{-1}}) \quad (1)$$

$$\mathrm{BAF} = \text{tissue } (\mathrm{ng\,g^{-1}dw})/\text{surface sediment } (\mathrm{ng\,g^{-1}dw}) \quad (2)$$

$$\mathrm{BSAF} = ((\text{tissue } (\mathrm{ng\,g^{-1}dw})/f_{(\mathrm{lip})})/(\text{sediment } (\mathrm{ng\,g^{-1}dw})/f_{\mathrm{oc}})) \quad (3)$$

where $f_{(\mathrm{lip})}$ is the fraction of lipids in the tissue (ng g^{-1} dw) and f_{oc} is the fraction of organic carbon in the sediment (ng g^{-1} dw).

2.6. Partition Characteristics of PBDEs and PAEs. To understand the partitioning coefficients of PBDEs and PAEs between aqueous and sediment phases (or SPMs), the relationship between organic carbon normalized partition coefficients (K_{oc}) and octanol−water partition coefficients (K_{ow}) was analyzed. In this regard, K_{oc} was calculated as the formula[34,40]

$$K_{\mathrm{d}} = 1000 \times C_{\mathrm{s(ng\,g^{-1}dw)}}/C_{\mathrm{aq\ (ng^{-1}L)}} \quad (4)$$

$$K_{\mathrm{oc(cm^3g^{-1})}} = K_{\mathrm{d}} \times 100/f_{\mathrm{oc}} \quad (5)$$

where C_{s} and C_{aq} are the concentrations of PBDEs and PAEs in the surface sediment (or SPMs) and seawater, respectively, and f_{oc} is the % total organic carbon (TOC) in the sediment. Then, the correlation between field-based $\log K_{\mathrm{oc}}$ (organic carbon (sediment)−water) and $\log K_{\mathrm{oc}}$ (organic carbon (SPM)−water) of PBDEs and PAEs and their $\log K_{\mathrm{ow}}$ (octanol−water) were also estimated.

2.7. Statistical Analysis. The normality of distributions of POP-type contaminant concentrations in environmental samples was tested by the Shapiro−Wilk test. Moreover, to generate the correlation matrix, Pearson's correlation coefficient test and Spearman's correlation coefficient test were performed on normally and not normally distributed data, respectively. To distinguish differences of PBDE and PAE accumulation in biota and abiotic matrixes, analysis of variance (one-way analysis of variance (ANOVA)) was conducted. Hierarchical data clustering was analyzed by assessing the high similarity scoring by R-software (R Development Core Team,

https://doi.org/10.1021/acs.est.0c08730
Environ. Sci. Technol. XXXX, XXX, XXX−XXX

Vienna, Austria). The odds ratios (ORs) were estimated using the statistical software IBM SPSS Statistics (19.0) and OriginPro 2020b (9.75). To generate network models (NA) with highly interconnection-specific pathways, Gephi software (ver. 0.9.2) was used. The classification methods of Kohonen's self-organizing map (SOM) for artificial neural network (ANN) modeling were operated by MATLAB software (Version: R2019b). Variations were considered significant with $p < 0.05$. Statistical analyses were performed using the R programming language (R Development Core Team, Vienna, Austria) and OriginPro (Version: 2019b, 9.65). Additional details on statistical analyses are provided in the SI Appendix, Supporting Information.

3. RESULTS AND DISCUSSION

3.1. Natural Environmental Variables. In terms of the water quality assessment, variations of the bulk parameters of pH, dissolved oxygen (DO), and turbidity of water across sampling sites ST1 to ST8 ranged from 6.49 to 7.80, 5.95 to 7.65 mg L^{-1}, and 75.02 to 105.01 NTU, respectively ($p < 0.05$) (Figure S1). Other factors listed in Figure S1 were significant predictors for the ST1 (BOD, TOC, and NO_3^{-1}) and ST2 (PO_4^{-3}). The mean concentrations of BOD, TOC, NO_3^{-1}, and PO_4^{-3} of the surface water were 4.76−7.65 mg L^{-1}, 1.18−0.78 mg g^{-1} dw, 0.59−1.95 mg L^{-1}, and 0.20−0.74 mg L^{-1}, respectively (Figure S1). This result revealed that the chemobiological properties of seawater and nutrients of the Larak coral reef ecosystems were lower than the EPA-recommended surface water quality criteria.[42,43] These regional productions can be affected by the hydrography of the Persian Gulf, the proximity of the Larak Island to the Strait of Hormuz, and the dynamics of nutrient circulation between the Gulf of Oman and the southern Persian Gulf.[44] Additional details on the occurrence, spatial distribution, and quantification of PBDEs/PAEs in seawater (SW), the surface sediment (SS), and suspended particulate matters (SPMs) from the Larak Island abiotic matrixes are provided in the SI Appendix, Supporting Information.

3.2. Bio-chemoenergetics-Originated Coral Bleaching: The Synergistic Effects of Summer Bleaching Events and POP-Type Toxicants. Coral bleaching is a recurring cellular life/death balance phenomenon caused by heat, UV radiation, and chemical contaminants in reef regions around the globe.[4,45] Figure S2 provides examples of MODIS-Aqua Level 3 with daily, weekly, and monthly SST thermal infrared (IR) products (min = 26.1 °C, max = 36.8 °C; mean = 33.45 °C), concomitant with a positive anomaly between 1 and 3 °C, over an approximate one-and-a-half-month period (July 2015) in the Persian Gulf, Larak Island. The daily averaged NASA's OMI Aura satellite-retrieved UVI data taken over the summer (July 2015 at 931 W m^{-2}) with the highest UV irradiance at local noon and sunshine hours (05:00 to 06:00 local time, July 15, 2015) was 50 ± 2 W m^{-2} UVA and 1.9 ± 0.1 W m^{-2} UVB. Global horizontal irradiance (GHI) maps, as shown in Figure S3, highlight the SST ≥ 34 °C,[46] solar insolation ≥ 275 w/m,[2,47] net radiation ≥ 168,[48] and UVI > 11[30] for the Persian Gulf, including Larak Island. Due to the geographical location of the Persian Gulf coral reef ecosystem in the global sunbelts, the forecasted summer incoming UV/solar radiation is emphasizing the high risk of corals succumbing to the negative aspects of UV/heat overexposure (e.g., bleaching and damage protection).[46,47,49] This has been clarified as a signature of global warming emergency. Persian Gulf has warming rates of 0.4 °C SST per decade (2-fold the global average) since the 1980s.[50] Riegl et al.[46] suggested that the coral bleaching threshold in the Persian Gulf is triggered by the maximum temperatures of >35.7 °C on a typical summer day and/or longer exposure to sublethal temperatures of 33−35 °C with marine heatwave conditions (e.g., large-scale mass mortality events of *Acropora* spp. in summers of 1996 and 1998).[51] At this time, the mostly stress-tolerant hardbottom reef communities of brain and mound/boulder corals (e.g., mainly faviids and poritids) are dominant in these areas.[52]

The results from the direct field observations of inter-ST differences at Larak Island in 2015 (Figure 1) confirmed that about 75% of coral colonies (100% of hard corals) were affected by bleaching (thermosensitive). While the unaffected corals were soft corals at ST7 and ST8, sporadic partially discoloration of a few colonies was observed. In view of intergenus differences, *Platygyra* spp. was the only genera with the most bleached colonies (16.20%); *Favia* spp. and *Porites* spp. had the percentage of bleached colonies of 13.97 and 9.85%, respectively; and in contrast, the highly susceptible corals such as *Acropora* spp. were affected by bleaching (12.32%), as previously reported by Kavousi et al.[53] Notably, *Sinularia* spp. and *Sarcophyton* spp. were recorded as thermotolerance genotypes since they recovered better than other studied taxa.[54] Differences in taxa photosensitization may be caused by SST/UVR/POPs and be due to the longer duration of overlapped exposure, the formation rate of water-soluble fractions of POPs by photooxidation, and elevated hazard oxidative transformation/DNA cross-linking products within the coral cells.[8,55] However, variance partitioning in our study indicated that anthropogenic POP-type pollutants alone contributed larger (10.8% (PBDEs) and 7.7% (PAEs)) than natural variables (5.9%) to the coral bleaching variation in the coastal regions of the Larak Island (Figure S4). Though the Persian Gulf coral physiology is capable of adapting to climatic extremes[46,56,57] and coastal development,[58] the loss of coral reefs[47,53] only becomes challenging if bleaching and necrosis damages are subjected to a subset of stressor-induced photosynthesis perturbation, such as organic and/or micro-plastic-related contaminants.[5,8,46] These pollutants can be targeting photosensitization/photomodification to result also in genotype-specific toxicity exacerbated up to 7.2-fold in shallow reef habitats.[8]

In corals, however, Bainbridge et al.[59] also alluded that SPM (<63 μm) export along the "ridge-to-reef" continuum mitigated solar damage. Dominant turbid waters in coral genera at 3−5 m depth of coral reefs have suggested that brain or elkhorn assemblages are more susceptible to heat/post-bleaching destructive stresses.[53] In this regard, the highest ∑PBDEs/PAEs levels were observed in the order of SPMs > SS > SW in the Larak Island. Moreover, SPMs are not easily removed from the coral surface; therefore, they attenuate sunlight, alter the spectral composition, and may act as POP vectors in the water column. Hence, all of these can reduce coral photosynthetic and oxygen products, thereby causing colony degradation or even bleaching.[59]

3.3. Scenarios of Species-Specific Coral Compartmentalization Breakdown by PBDE/PAE Exposure. *3.3.1. Coral Skeletons.* The $\sum_{18}$PBDEs and $\sum_{13}$PAEs in the Larak Island hard and soft coral skeletons are summarized in Table S1. The skeletal ∑PBDEs and ∑PAEs showed an average of 35.66 ± 9.58 and 6.47 ± 6.47 ng g^{-1} dw per coral, respectively. ∑PBDEs and ∑PAEs were found at the highest

https://doi.org/10.1021/acs.est.0c08730
Environ. Sci. Technol. XXXX, XXX, XXX−XXX

levels of 51.02 and 19.66 ng g^{-1} dw in the skeleton of *P. lutea* and *F. speciose*, respectively, followed by *P. daedalea* for both POPs (Table S1). Conversely, the lowest levels were in *A. robusta* (∑PBDEs: 25.25 ± 4.57 ng g^{-1} dw) and *P. lutea* (∑PAEs: 3.01 ± 1.25 ng g^{-1} dw) (Table S1).

As a respondent to abiotic factors, BDE209 (mean: 2.44 ng g^{-1} dw, 1.14% of ∑PBDEs) in *Acropora* spp. (*A. valida* > *A. robusta*) and BDE138 (mean: 3.37 ng g^{-1} dw, 1.57%) in the order *P. lutea* > *P. daedalea*> *F. speciose* > *F. favus* are the most common congeners in skeletons of scleractinian corals ($p < 0.05$), followed by BDE190 (2.53 ng g^{-1} dw), BDE47 (2.51 ng g^{-1} dw), BDE85 (2.51 ng g^{-1} dw), BDE100 (2.29 ng g^{-1} dw), and BDE183 (2.27 ng g^{-1} dw) (Figure S5A). For PAE congener profiling, the highest level for all hard corals was found for BBP (mean: 2.36 ng g^{-1} dw, 4.19% of ∑PAEs) in the order *F. speciose* > *F. favus* > *P. daedalea*, followed by DBP (mean: 1.23 ng g^{-1} dw, 2.19%) > DEHP (0.98 ng g^{-1} dw 1.74%) ≥ DEP (0.96 ng g^{-1} dw, 1.70%) ($p < 0.05$) (Figure S5B).

According to the significant differences in ∑BDE209 and ∑BBP between ST1 and ST5 and the other STs, the spatial variation of emerging POP-type contamination in the Larak coral reefs depends on the sampling sites. To the best of our knowledge, no EPA-IRIS RfD, SRCeco, and/or ERLs have been established for POP bioaccumulation in cnidarians; therefore, these ∑PBDEs/PAEs levels in skeletal and other coral compartments are herein discussed for the derivation of health risks.

The result for coral skeleton-phase PBDE/PAE-bioaccumulation (particularly those with $K_{ow} > 5$; $p < 0.05$) showed the general POP level alignment with relative trends in log K_{ow} and their significant distribution across the eight sites (Figure S6). For hydrophobic PBDE/PAE compounds, the paired log BSAFs and log BCFs and log K_{ow} for the Larak Island showed significant positive correlations ($p < 0.05$) between coral-skeleton-adsorbed POPs and their octanol−water partition coefficients in the ambient environment (Figure S6). The average log BSAFs and BCFs in the coral skeletons were 1.30 ± 0.07 and 1.59 ± 0.07 log unit for the detected 18 PBDEs and 1.27 ± 0.19 and 1.58 ± 0.22 log unit for the detected 13 PAE congeners, respectively (Tables S2 and S3). Based on the classification of the United Nations Environmental Program (UNEP), the criterion of a chemical for aquatic species has been posed >5000 L kg^{-1} (i.e., log BAF = 3.7).[60,61] Therefore, it seems that estimated levels of bioaccumulative PBDE/PAE congeners (Tables S2 and S3) in the Larak Island coral skeletons are not potentially harmful. Since these POP-type congeners are less water-soluble and can easily adsorb onto coral macrostructural aragonite/$CaCO_3$ sections, the reasons may be found in skeleton cavities' dependency both through a different partitioning across the abiotic matrixes and variation of the coral excretion rate.[62]

3.3.2. Coral Tissues. The mean values of ∑PBDEs and ∑PAEs in the Larak Island coral tissues were found in the range 66.26 ± 21.42 ng g^{-1} dw and 34.97 ± 26.10 ng g^{-1} dw, respectively. As shown in Table S1, the maximum levels of ∑PBDEs and ∑PAEs (ng g^{-1} dw) were detected in soft coral tissues of *S. trocheliophorum* (107.51 and 103.49, respectively), followed by *S. compressa* (86.77 and 77.11) and hard coral *P. lutea* (74.03, PBDEs) and *F. speciose* (35.89, PAEs), whereas the minimum level was in *A. valida* (46.11, PBDEs) and *P. daedalea* (4.43, PAEs). Therefore, PBDEs/PAEs have been detected in tissues of various coral species, suggesting the occurrence of their transfer via food, natural pathways (i.e., seawater/sediment/SPMs), and/or plastic additives in the Larak Island corals. Among biota, regardless of the coral inter- and intraspecies differences in POP-uptake/depurations and/or environmental sites, the morphology of corals plays a key role in their distinct accumulating responses to pollutants. In this regard, reef flat corals (i.e., *P. lutea*) and massive broad soft corals with larger areas were more susceptible to PBDE/PAE enriching than foliaceous/branched species (i.e., *Acropora* spp.).[1]

In the majority of coral species tissues, the BFR congener BDE209 had the highest value (ng g^{-1} dw) (mean: 5.70, 1.07% of ∑PBDEs) in the order *S. compressa* (12.48) > *P. lutea* (7.47) > *A. valida* (4.62) > *F. speciose* (4.58) ≥ *P. daedalea* (4.58), followed by BDE47 (mean: 4.82, 0.90%, max: 4.09 in *F. favus*) and BDE138 (mean: 4.60, 0.86%, max: 10.96 in *S. trocheliophorum*) ($p < 0.05$) (Figure S5A). Besides the results mentioned, the ratios of BDE99/BDE100 (R2) for coral species were found to be ≥1, while the ratios of BDE99/BDE47 (R3) were found to be slightly lower than 1 (Figure S7). This result suggests that trophic-level-dependent biotransformation of BDE99 into BDE47 would contribute to the dominance of BDE100 and biomagnification of BDE47 in the Larak Island corals.[63]

Regarding PAEs, BBP (mean: 7.65 ± 2.78 ng g^{-1} dw, 2.73% of ∑PAEs) was found in the maximum levels in the order *S. trocheliophorum* (23.29 ng g^{-1} dw) > *S. compressa* (16.55 ng g^{-1} dw) > *F. speciose* (7.65 ng g^{-1} dw) > *F. favus* (4.97 ng g^{-1} dw) (Figure S5B). Overall, the relative abundance of different PAE congeners (ng g^{-1} dw) was as follows: BBP (7.65) > DBP (5.48) > DEHP (4.26) > DEP (3.97) > DIBP (2.72) > DPP (1.48) ($p < 0.05$) (Figure S5B). The discrepancy results regarding PBDE/PAE congener levels between coral species may stem from differences in their metabolic/detoxification activities.[64]

Herein, a positive correlation was observed between the log K_{OW} and the log BSAFs/log BCFs for 18 PBDE and 13 PAE hydrophobe congeners in eight coral tissues (r^2 ranged from 0.31 to 0.51, $p < 0.05$) (Figure S6). The results of coral tissue BSAFs and BCFs for PBDEs/PAEs are shown in Tables S2, S3, and Figure S6. The average levels of log BSAFs and BCFs were 1.23 ± 0.05 and 1.51 ± 0.05 log unit of individual PBDEs and 1.33 ± 0.09 and 1.64 ± 0.13 log unit of individual PAEs, respectively (Tables S2 and S3). Based on the ECA and WWF classification for POP bioaccumulation (PB),[60,61] PBDE/PAE congeners are not considered as "potentially bioaccumulative" (3.3 < PB < 3.7) in the Larak Island coral tissues (Tables S2 and S3).[35,62]

3.3.3. Zooxanthellae. The ∑PBDEs (mean: 82.05 ± 28.27 ng g^{-1} dw) per zooxanthellae had the same trend/range as coral tissues (soft corals> hard corals), in the order *S. trocheliophorum* (max: 141.85 ng g^{-1} dw) > *S. compressa* > *P. lutea* > *P. daedalea* > *F. speciosa* > *F. favus* > *A. valida* > *A. robusta* (min: 55.55 ng g^{-1} dw) (Table S1). Conversely, for ∑PAEs in zooxanthellae (mean: 20.14 ± 12.65 ng g^{-1} dw), the reverse trend was observed compared to that in tissues: *F. speciosa* (max: 47.34 ng g^{-1} dw) > *F. favus* > *P. daedalea* > *A. robusta* > *S. trocheliophorum* > *S. compressa* > *A. valida* > *P. lutea* (min: 6.95 ng g^{-1} dw) (Table S1).

Among all coral species, BDE209 had the highest value (mean: 7.11 ng g^{-1} dw, 1.08% of ∑PBDEs, max: 16.09 in *S. compressa*), except in *P. daedalea*, followed by BDE47 (mean: 5.98 ng g^{-1} dw, 0.91%, max in *F. favus*) and BDE138 (mean:

https://doi.org/10.1021/acs.est.0c08730
Environ. Sci. Technol. XXXX, XXX, XXX−XXX

4.23, 0.64%, max: 15.38 in *S. trocheliophorum*) (Figure S5A). As shown in tissues, the relative abundance of PAE-zooxanthellae congeners was in the order of BBP (mean: 4.18 ng g^{-1} dw, 2.59%) > DBP (2.84 ng g^{-1} dw, 1.76%) > DEP (2.28 ng g^{-1} dw, 1.41%) > DEHP (2.21 ng g^{-1} dw, 1.37%) (Figure S5B).

The $\sum_{18}$PBDE/$_{12}$PAE pattern was zooxanthellae (extreme levels of BDE209/47/138) > coral tissues (BDE209/47/138) > coral skeleton (BDE209/138) in the Larak coral reefs. The density of zooxanthellae (DZ) (mean: 157816.42 zooxanthellae cell cm^{-2}) in corals from the Larak Island had a significant positive correlation with $\sum_{17}$PBDEs (r^2 = 0.42, p < 0.05), but negative significant correlations were found among these corals' DZ and $\sum_{13}$PAEs (r^2 = 0.87, p < 0.05) (Figure S8A). The maximum mean DZ values (z-cell cm^{-2}) were reported for *P. lutea* (253800), followed by *F. speciose* (236880) and *A. robusta* (217140), whereas the minimum values were reported for *S. trocheliophorum* (969) (Figure S8B). The data are comparable to those of the Mediterranean scleractinian corals.[65] The average levels of chlorophyll *a* (μg Chl-*a*·cm^{-2}) and c_2 (μg Chl-C_2·cm^{-2}) in corals from the Larak Island were 932 (ranged from 517 (*P. lutea*) to 1404 (*S. trocheliophorum*); Chl-*a*: soft corals > hard corals) and 2192 (from 398 (*S. trocheliophorum*/*S. compressa*) to 3644 (*F. favus*); Chl-C_2: hard corals > soft corals), respectively (Figure S8B). Values of the ratio of Chl-*a*/Chl-C_2 (R1) as an indicator of dinoflagellate photoacclimation in hard corals (max R1: 0.87 in *A. valida* and *P. lutea*) were higher than those in soft corals (min R1: 0.61) (Figure S8C). The reverse trend was observed in DZ-to-Chl-*a* content in examined corals, indicating that this could be a not common pattern because both soft coral species and some of the hard corals with the highest Chl-*a* concentration had the minimum density of *Symbiodinium* (Figure S8B) and maximum levels of $\sum_{17}$PBDE/$_{13}$PAE accumulation (Table S1). In this regard, Tolleter et al.[56] suggested that the dark-bleaching mechanisms in hard corals during marked short-term warm-water events could be caused by the expulsion of zooxanthellae and reduction in the DZ in the host tissue at night and might be operating synergistically with day heat/solar-bleaching factors. In PB, however, the symbiotic relationship between algae and corals can be an important route for POP uploading in coral tissues and zooxanthellae with larger surface areas having a higher uptake efficiency for POPs,[38] but through z-expulsion as a consequence of a decrease in Chl-*a* and PP contents, this pathway was suppressed. Therefore, the nonlinear correlation of POP levels and Chl-*a*/Chl-C_2 indicated that coral tissue PB is probably a complicated process; algal PB is not the main source; and direct sorption from feeding, water, and sediments could affect coral PB.[66] Additionally, following the alcyonacean soft coral (i.e., *Sinularia spp.*) bleaching, the zooxanthellae loss resulted in a significant short-term adjustment of the tissues' secondary metabolites such as flexibilide (cytotoxic/antimicrobial) and sinulariolide (algaecide) to suit specific needs for recovery of the algal overgrowth to baseline levels.[67] Furthermore, compared to their unbleached counterparts, in bleached corals, production of specific algaecides leading to higher protection was gained through the recurrence of bleaching.[67]

The differences in Symbiodiniaceae soft coral communities may also play a key role in coral susceptibility to cumulative bleaching events.[68] Soft corals such as *Sinularia spp*. released the greater number of their symbionts during bleaching events, based on their clade type of Symbiodinium, but were less susceptible to elevated heat stress (i.e., SST ≥ 34 °C) than other less-resistant soft corals (i.e., *Xenia spp.*).[69]

From a toxicology point of view, paired log BASF/log BCF and log K_{ow} of zooxanthellae for $_{18}$PBDE/$_{12}$PAE-individuals exhibited significant positive correlations (r^2 ranged from 0.32 to 0.52, p < 0.05) (Figure S6). Furthermore, according to the results of calculated bioaccumulation factors for POPs in zooxanthellae (Tables S2 and S3), the mean values of log BSAFs and BCFs were 1.70 ± 0.02 and 1.96 ± 0.02 log unit (PBDEs) and 1.69 ± 0.11 and 2.03 ± 0.19 log unit (PAEs), respectively (Tables S2 and S3). Although there is no consensus with respect to hazardous levels of PB,[60,61] this trend indicated the degrees of heterotrophic/autotrophic POP trapping by the symbiotic zooplankton of Larak coral reefs.[65] Massive corals were often fat-enriched invertebrates.[70] In this regard, the mean concentration of the lipid content (all corals: 3.16 ± 1.57 mg g^{-1}) for hard and soft corals was 2.48 and 5.19 mg g^{-1}, respectively, harboring significant highest values in *S. compressa* and the lowest values in *P. daedalea* (Figure S8B). As shown in soft corals (Figure S8B, Tables S1−S3), the distinct PB capacity (particularly the POP congener with K_{ow} > 5) in coral biological compartments (tissues/zooxanthellae) is affected by the lipid content based on the cnidarian xenobiotic metabolism pathways.[8,65,71]

3.4. Glimpse of the POP-Bleaching Biomarkers: Species-Specific Mucus Partitioning of PBDEs/PAEs in Corals. Coral mucus is a key diagnostic tool for detecting marine water quality and hazard acceptability thresholds for sustaining healthy corals.[1,72] Herein, the levels of the net bioaccumulation of PBDEs/PAEs in Larak Island coral mucus[1] (Figures 1 and S5A,B) led to a distinct decline in net hermatypic coral photosynthetic activity[20,73] (Figures 1 and S8) and symbiosis collapse in bleached corals. In this regard, our data suggest that the $\sum_{18}$PBDE and $\sum_{13}$PAE concentrations in mucus were significantly higher in the ahermatypic corals such as *S. trocheliophorum* and *S. compressa* (ranged from 50.5 to 48.4% of total PBDEs, mean: 254.50 ± 0.31−200.92 ± 0.11; 58.3% of total PAEs, 166.85 ± 0.38−129.32 ± 0.30 ng g^{-1} dw, respectively) than in the hermatypic corals such as *A. robusta*, *A. valida*, *P. lutea*, and *F. favus* (45.8−34.9% of $\sum$PBDEs, mean: 152.15 ± 0.41−113.12 ± 0.31; 58.9−42.7% of total PAEs, 64.38 ± 0.12−51.50 ± 0.18 ng g^{-1} dw, respectively) (Figures 1 and S5A,B). The coral tissue/mucus taxa-specific differences in POP enrichment were previously reported in the order of massive corals > foliaceous corals > branched corals, with an exception for Acroporidae.[1] This comparison may also be affected by different coral growing habitats,[1] microbiome communities of mucus,[74] symbiont type,[75] synergistic effects of environmental stress,[76] and reef urbanization and disturbances.[64,77]

In contrast, across bleached corals of Larak Island reefs, mean values of $\sum_{18}$PBDEs and $\sum_{13}$PAEs demonstrated the highest levels (17.2−16.0% of the total, mean: 46.57 ± 0.11 ng g^{-1} dw; 15.2−14.6% of the total, 21.02 ± 0.15 ng g^{-1} dw, respectively) in the skeleton of *P. daedalea* and *F. speciosa* (Figure 1). On the other hand, there are correspondingly lowest levels (28.6−22.9% of the total, mean: 46.57 ± 0.11; 43.5−24.6% of the total, 45.44 ± 0.11 ng g^{-1} dw, respectively) of POP-type accumulation in mucus and high levels (59.8% of the total, mean: 165.25 ± 0.32; 60.6% of the total,102.89 ± 0.61 ng g^{-1} dw, respectively) in tissues of unbleached *P. daedalea* and *F. speciosa*, respectively (Figures 1 and S5A,B). Specifically, in the coral-pollutant logistic regression model, the

https://doi.org/10.1021/acs.est.0c08730
Environ. Sci. Technol. XXXX, XXX, XXX−XXX

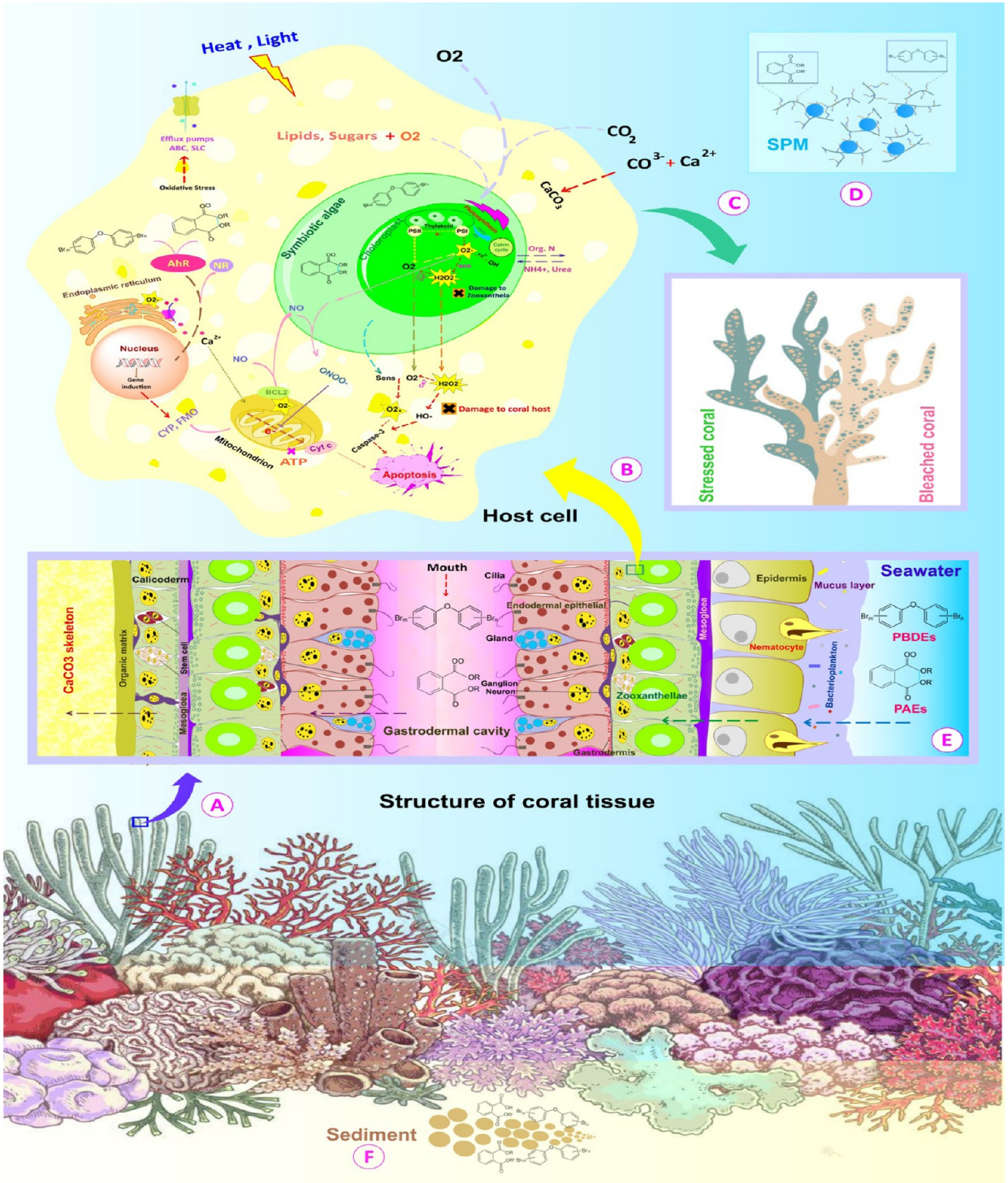

Figure 2. Schematic cellular-based mechanistic diagram representing the coral toxicokinetics end points for environmental PBDE/PAE-originated bleaching events. Detailed descriptions are found in SI Appendix, Supporting Information.

effect estimates were odds ratio (OR) ≥ 1 (95% confidence interval, $p < 0.05$) for an increase in PBDE and PAE levels (a 14.45 and 11.76% increase in exposure, respectively). These odds ratios indicate that there is an association between an increase in the PBDE and PAE levels and the occurrence of coral bleaching (Figure S9).

Chronic exposure of hard corals to a chemical toxicant can combine and interact with other sublethal environmental stresses, such as heat/photooxidation of PBDEs/PAEs by UVA at 1−2 °C above the mean Larak Island SST (>36.0 °C in summer).[45,54,55,78] In this case, the coral bleaching commonly occurs likely due to the following PBDE/PAE accumulation pathway: POPs induce tissue-specific apoptosis and enhance the release of zooxanthellae; as a consequence, the loss of coral tissue and massive mucus hanging from the coral skeleton will occur, and finally, POPs are transferred/biomineralized by lipid vesicles (or by phospholipids, free fatty acids, and sterol esters) to $CaCO_3$ as the final repository of metabolites[65] (Figure 2).

Therefore, in parallel, high levels of POPs in the skeleton of bleached corals reflect the high POP levels in coral

https://doi.org/10.1021/acs.est.0c08730
Environ. Sci. Technol. XXXX, XXX, XXX−XXX

biocompartments. The estimates in ST4 and ST5 based only on the net fixed carbon/nutrient recycling (TOC, NO_3^{-1}, and PO_4^{-3}) by older undissolved coral mucus[79] for the Larak Island reef sediment showed significantly lower concentrations compared to those in ST7 and ST8 (soft coral residence) (Figure S1). However, controversially, no bleached soft corals were recorded in ST7 and ST8, despite their highest accumulated levels of ∑PBDEs/PAEs. Given that these sites are in the eastern of Larak Island (Figure 1) and far from the coastal water of Hormozgan Province, Qeshm Island, and Strait of Hormuz, it seems that these STs are less subjected to overfishing[80] and the loss of dynamic natural coral covers communities such as fish, molluscs, and macroalgae.[81] Others have argued that these offshore stations may be more affected by the tropical summer southwest monsoon along the Iranian coastal water of the Gulf of Oman[44] that may bring the biggest extent of POP-type pollutants from other Middle-East countries.

In view of molecular dynamics (MD) of toxins, PAEs and PBDEs have high hydrophobicity and low solubility based on the wide range of octanol/water partition coefficients (log K_{ow} = 1.6−8.2 and 5.74−8.27, respectively) and planar (benzene ring) or near-planar moieties.[82,83] Thus, due to the strong influence of surface charge density and size of the PAE/PBDE molecules, they have a viability of intercalation into smectite interlayer regions (clay/silicate-organic systems).[82] In aqueous suspensions of the smectite clay (such as SPMs), the photooxidation (λ, 300−800 nm) rate of the aromatic organic pollutants (AOPs) is significantly enhanced and correlates to the saltwater and freshwater interface. Cl^-, Br^-, and I^- have relatively contributed to the steady-state singlet oxygen $[^1O_2]$ss quencher, so the predictive photoprocessing of particle-bound-AOPs falls off as rapidly as they are transported into seawater.[84] As shown in Figure S10, the photocatalytic degradation of PBDE (BDE47 to BDE28 and BDE17) and PAE (DEP to MEP and OH-DEP) congeners under UV light,[11,54,78,85,86] dependent on the season (mainly summer) as July 2015, Persian Gulf, was elevated and there was a direct induction to reactivity/stability of AOPs, which can result in the generation of more toxic byproducts (such as polybrominated dibenzofuran, PBDF) than its parent one.[6,85,87] For an overview, congeners BDE209 (as a heavier congener, range 10.68−2.27 ng g^{-1} dw), BDE47 (6.99−3.08 ng g^{-1} dw), and BBP (9.20−1.09 ng g^{-1} dw) in the skeleton, mucus, tissue, and zooxanthellae components of both types of corals were detected at the highest levels and found to be more recalcitrant toward selective chemo/biodegradation[22] (Figure S5A,B). Additionally, a positive correlation (r^2 = 0.77, p < 0.01 and r^2 = 0.79, p < 0.01, respectively) between coral mucus log K_{ow} and log BAFs for PAE and PBDE congeners was observed.[1] The recorded log BSAFs and BCFs in coral mucus were 1.92 ± 0.06 and 2.17 ± 0.05 log unit of PBDEs and 2.22 ± 0.15 and 2.54 ± 0.22 log unit of PAEs, respectively (Tables S2 and S3), thus significantly higher than in zooxanthellae, while those in bleached corals were in the range of 1.44 ± 0.07 and 1.69 ± 0.08 log unit of PBDEs and 1.47 ± 0.24 and 1.79 ± 0.34 log unit of PAEs (<3.3 PB unit), respectively (Tables S2 and S3).

These results may suggest a different PBDE/PAE accumulation mechanism in the mucus of coral species. Given that PBDEs/PAEs do not seem to be bioaccumulative chemicals, their partial solubility in biological fluids, plastic debris leaching/weathering, and solid-phase absorbance affinity may be facilitating their collectivity in coral biocompartments.[33,35,62,82] The underlying mechanism to explain this congener bioaccumulation is in key suspension feeding of coral taxa and their adhesive mucus filaments' potential to capture fine particle-bound AOP matter and incorporate their bacterioplankton (Figure 2) for biodegradation of other AOPs.[1,74,88−90] The composition of mucus in soft/hard corals includes energy-rich compounds such as carbohydrates, glycoproteins (mucins), and lipids (wax esters/triglyceride/free fatty acids),[91,92] mainly derived from primary production (PP) of algal endosymbionts and with higher accumulation potential to lipophilic AOP compounds.[1] The cellular metabolic regulation of mucus in corals is affected by heat, light, and UV and also by the adsorption rate of the chemical particulate matter[1,54,91−94] (Figure 2). Hereupon, these mucosal AOP loads also reach tissue/zooxanthellae and induce chemo/phototoxicity and symbiotic disruption.[55,95,96] So far, PBDEs/PAEs have been demonstrated to disturb carbon-fixation cycles[73,93] and the normal symbiotic relationship between a symbiont and host,[93] provoking damage to cell organelles of algae (cell membranes, chloroplasts, protein rings),[97] and be genotoxic/mutagenic/cytotoxic (DNA-PBDE/PAE adduct) in the microenvironment.[93,98,99] Indeed, the effect of short-period BDE47 exposure (1 μg L^{-1}) to the marine sponge *Haliclona cymaeformis* caused a substantial decrease in the abundance of symbiont *Ectothiorhodospiraceae* (autotrophic bacteria/sulfur-oxidizing) and the enrichment of heterotrophic bacteria (*Clostridium*).[93] Similarly, herein, species of reef-building corals challenging a rapid uptake of ∑PBDEs/PAEs in their tissues had minimum levels of lipids (mean: 1.3 ng g^{-1} dw), endosymbiont density (mean: 120 000 z-cell cm^{-2}), and pigmentation (chlorophyll-*a* content ranged from 517 to 719 pg $cell^{-1}$) (Figure S8) compared to soft coral species (i.e., *S. trocheliophorum* and *S. compressa* with high levels of lipid content and photosynthetic activity and no record of bleached specimens). In a previous study, the levels of mycosporine-like amino acids (MAAs) (e.g., palythine) were significantly higher in the zooxanthellae symbionts of *Sinularia maxima*. MAAs act as natural sunscreens (absorb the UV) and are produced in the shikimate biosynthetic pathway by primary producers.[100,101] Despite several chronic factors (i.e., symbiont types, temperature, turbidity, SPMs, etc.) that may have contributed to differences in coral taxonomic bleaching susceptibility,[64] our results suggest that soft coral resistance to PBDE/PAE stress may be remarkably promoted in tissue-mucus partitioning. The diverse biochemical constituents and specific defensive metabolite production[64,77,100,101] by soft corals at Larak Island may be an inducible response to increasing bleaching stress. This finding confirmed that coral response to PBDE/PAE-originated bleaching was different among taxa.

Given that the released coral mucus "floes" acts as a biocatalytic mineralizing filter and biotrapper for AOP (PBDEs/PAEs) compounds from ambient seawater and direct drifts on the surface reef sediment (see the levels of ∑PBDEs/PAEs in environmental matrixes of Larak Island (S1−S8) (Figure S1))[79] and a contributor to coral reefs' top-bottom trophic pathways (efficiently assimilated carbon into high gross PP by zooxanthellae or microbial loop),[79,89,92,93] an alteration in the chemocomposition of mucus could be attributed to a putative functional biomarker for coral bleaching events in reef ecosystems.

3.5. Self-organizing Map (SOM) Clustering Analysis.

In SOM clustering analysis for similarities between coral-

https://doi.org/10.1021/acs.est.0c08730
Environ. Sci. Technol. XXXX, XXX, XXX−XXX

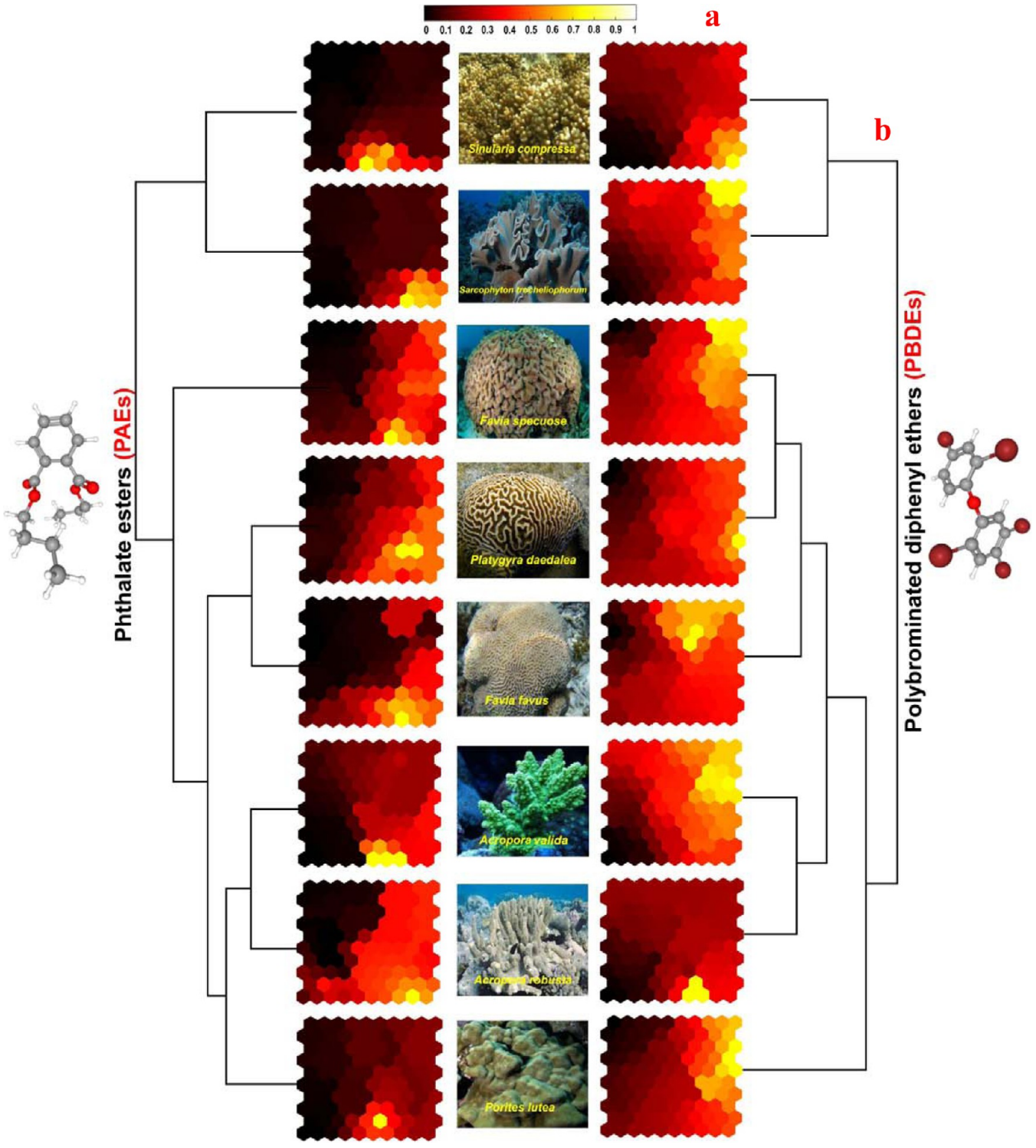

Figure 3. Clustering of the self-organizing maps (SOMs) for coral $\sum_{18}$PBDE and $\sum_{13}$PAE uptake in the Larak coral reef ecosystems. (a) Hierarchical clustering of the quantified 30 POP congeners in the "biota sample dimension". (b) Each tile within an SOM mosaic represents a minicluster of POPs with similar patterns across all genera of corals. The map unit shows the corresponding weighted distance (Euclidian distance). Tile's color indicates minicluster's average POP concentrations in each layer.

species-specific 30 POP-congener (PBDEs and PAEs) uptakes in the Larak Island, two main clusters, namely, "a" and "b" as soft and hard corals, respectively, were recognized. In this dendrogram, other subclusters exhibited high similar interaction patterns to POP-associated HCA in biota matrixes (Figure 3). The algorithm for training the SOM was performed on a matrix grid with 100 neighboring modules (10 × 10), quantization error (QE = 0.81), and topographic error (TE = 0.023). From the component planes (Figure 3), to recognize the differential internal correlations between the ∑PBDE/PAE patterns in the total body of coral species, all pairs of neighboring map units (node) with similar color emission corresponded to certain neurons through the grid. Recognizing the neurons of inner congeners related to coral-specific PBDE/

https://doi.org/10.1021/acs.est.0c08730
Environ. Sci. Technol. XXXX, XXX, XXX−XXX

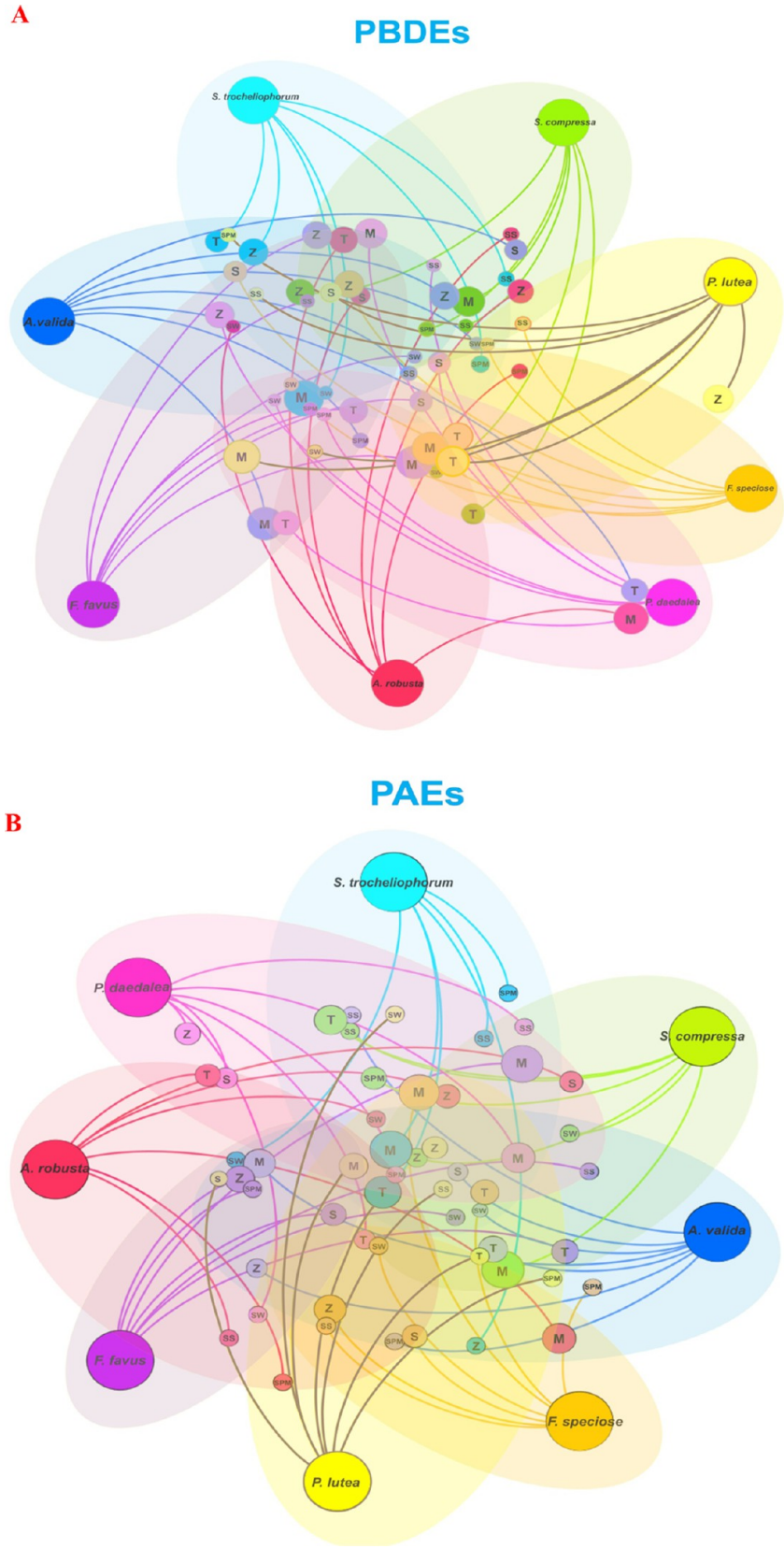

Figure 4. Network neighborhood analysis (NNA) of (A) ∑PBDE and (B) ∑PAE partitioning in coral components (skeleton (S), tissue (T), zooxanthellae (Z), and mucus (M)), and their specific environmental matrixes (surface sediment (SS), seawater (SW), and SPMs) to visualize the top-scoring nodes side by side in this in situ study (Spearman's $\rho > 0.6$ and $p < 0.01$). The connections between two nodes represent the correlation coefficient between them, and the size of each node is proportional to Spearman's correlation coefficients.

https://doi.org/10.1021/acs.est.0c08730
Environ. Sci. Technol. XXXX, XXX, XXX−XXX

PAE accumulation showed that the BDE209, BDE47, BDE28, BDE138, BBP, DBP, and DEP were determined as the most over-represented functional congeners in the total body of coral species, which can indirectly confirm the effect of photocatalytic degradation on coral POP congener profiles.[11,78,85,86] The similarity and categorization of coral ∑PBDE/PAE distribution in the same cluster of species SOM depended on their close squared Euclidian distance and their weight positions of neurons.

The clustering SOMs based on internal relationships between the congeners for both soft (*S. trocheliophorum*) and hard (*P. daedalea* and *F. speciosa*) coral species with a maximum level of PBDE and PAE (ng g^{-1} dw) uptake are trajectories in Figure S11A,B. The color-clustered SOM map, applying the *k*-means algorithm for the soft/hard coral components with their specific niche matrixes and based on the Euclidian distance between PBDE/PAE congeners, clearly shows distinguishable differences among BDE47, BDE100, BDE154, and BDE209 in *S. trocheliophorum* (Figure S11A) and BDE47, BDE138, BDE190, and BDE209 in *P. daedalea* (Figure S11B) as enriched functional PBDE congeners and BBP, DBP, DEHP, and DEP in *S. trocheliophorum* and BBP and DBP in *F. speciose* as over-represented functional PAE congeners. For map units, the corresponding weighted distance for POPs can signify their origin from the same cited sources. Moreover, Figure S11A,B shows differences in the chemical composition between coral tissues and abiotic media. Specifically, Figure S11A (soft coral) also presents the cluster results from coral tissue and zooxanthellae that are more similar to each other than SW, SS, or SPMs. Similarly, SW, SS, and SPMs are more similar to each other than to coral tissues and zooxanthellae.

3.6. Ecospecies-Specific Co-occurrence Network. To detect ecological coral-species-specific co-occurrence patterns conducted on PBDE and PAE distribution in the Larak Island environment matrixes, Pearson's and Spearman's algorithms were used to identify hub nodes and building, analysis, and interpretation of the co-occurrence network (Figure 4A,B).

Deciphering these network graphs, it was revealed that the high-level co-occurrence correlations were determined among ecospecies corals, especially for mucus, and SW in *S. trocheliophorum*; for zooxanthellae, tissues, and SPMs in *S. trocheliophorum*; for mucus, tissue, and SW in *P. lutea* and *F. speciosa*; for mucus, zooxanthellae, SPMs, and SS in *S. compressa*; for zooxanthellae and SW in *P. daedalea* (in exposure to PBDEs) (Figure 4A); for mucus, zooxanthellae, and SPMs in *F. favus* and *P. lutea*; for mucus, zooxanthellae, and SW in *A. valida*; for mucus, tissue, and SPMs in *S. trocheliophorum*; and for tissues and SS in *S. compressa* (in exposure to PAEs) (Figure 4B). The mucus had maximum significant co-occurrence correlations with all of the others, whereas the skeleton displayed relatively low co-occurrence correlations.

Among corals species, strong and significant positive correlations between *P. lutea*/*F. speciosa* and *P. daedalea*/*A. robusta*/*F. favus* in exposure to PBDEs and between *P. lutea*/*F. speciosa* and *S. trocheliophorum*/*S. compressa* in exposure to PAEs are suggestive of common sources for these common members of corals against anthropogenic PBDE and PAE pollutants (e.g., chemical industries or discharge of urban waste). Based on PBDE and PAE motif distributions in the Larak coral reef ecosystem, these two networks reflected the homologous relationship (Figure 4A,B). In this work, on the combined use of the co-occurrence network and SOM model, a robust approach was presented for analysis of more complex coral community interactions with POP-type pollutants.

■ ASSOCIATED CONTENT

Supporting Information

The Supporting Information is available free of charge at https://pubs.acs.org/doi/10.1021/acs.est.0c08730.

Satellite radiation products; analytical process and QA/QC; statistical analysis; key resource table; and occurrence, spatial distribution, and quantification of PBDEs/PAEs in the Larak Island abiotic matrixes (PDF)

■ AUTHOR INFORMATION

Corresponding Author

Alireza Riyahi Bakhtiari − *Department of Environmental Sciences, Faculty of Natural Resources and Marine Sciences, Tarbiat Modares University, Noor, Mazandaran, Iran*; Email: riahi@modares.ac.ir

Authors

Ali Ranjbar Jafarabadi − *Department of Environmental Sciences, Faculty of Natural Resources and Marine Sciences, Tarbiat Modares University, Noor, Mazandaran, Iran*; orcid.org/0000-0001-9106-1981

Sakineh Mashjoor − *Marine Pharmaceutical Science Research Center, Ahvaz Jundishapur University of Medical Sciences, Ahvaz, Iran*

Tiziana Cappello − *Department of Chemical, Biological, Pharmaceutical, and Environmental Sciences, University of Messina, Messina, Italy*; orcid.org/0000-0002-7790-6324

Complete contact information is available at: https://pubs.acs.org/10.1021/acs.est.0c08730

Notes

The authors declare no competing financial interest.

■ ACKNOWLEDGMENTS

This investigation was supported by the Academy of Environment Science, Tarbiat Modares University in Tehran, Iran.

■ REFERENCES

(1) Han, M.; Zhang, R.; Yu, K.; Li, A.; Wang, Y.; Huang, X. Polycyclic aromatic hydrocarbons (PAHs) in corals of the South China Sea: Occurrence, distribution, bioaccumulation, and considerable role of coral mucus. *J. Hazard. Mater.* **2020**, *384*, No. 121299.

(2) Baum, G.; Januar, H. I.; Ferse, S. C. A.; Kunzmann, A. Local and regional Iimpacts of pollution on coral reefs along the thousand Islands North of the Megacity Jakarta, Indonesia. *PLoS One* **2015**, *10*, No. e0138271.

(3) Roth, M. S. The engine of the reef: photobiology of the coral−algal symbiosis. *Front. Microbiol.* **2014**, *5*, 422.

(4) Brown, B. E.; Dunne, R. P. Coral Bleaching: The roles of sea temperature and solar radiation. In *Diseases of Coral*; Bruckner, A. W.; Downs, C.; Galloway, S. B.; Porter, J. W.; Woodley, C. M., Eds.; John Wiley and Sons: Hoboken, NJ, 2015; pp 266−283.

(5) Syakti, A. D.; Jaya, J. V.; Rahman, A.; Hidayati, N. V.; Razai, T. S.; Idris, F.; Trenggono, M.; Doumenq, P.; Chou, L. M. Bleaching and necrosis of staghorn coral (*Acropora formosa*) in laboratory assays: Immediate impact of LDPE microplastics. *Chemosphere* **2019**, *228*, 528−535.

(6) Wang, R.; Tang, T.; Lu, G.; Huang, K.; Chen, M.; Tao, X.; Yin, H.; Dang, Z. Formation and degradation of polybrominated dibenzofurans (PBDFs) in the UV photolysis of polybrominated diphenyl ethers (PBDEs) in various solutions. *Chem. Eng. J.* **2018**, *337*, 333−341.
(7) Tian, C.; Pan, X.; Luo, Y.; Ebinghaus, R.; et al. Occurrence and spatial distribution of organophosphate ester flame retardants and plasticizers in 40 rivers draining into the Bohai Sea, north China. *Environ. Pollut.* **2015**, *198*, 172−178.
(8) Nordborg, F. M.; Flores, F.; Brinkman, D. L.; Agustí, S.; Negri, A. P. Phototoxic effects of two common marine fuels on the settlement success of the coral *Acropora tenuis*. *Sci. Rep.* **2018**, *8*, No. 8635.
(9) Ashok, A.; Kottuparambil, S.; Høj, L.; Negri, A. P.; Duarte, C. M.; Agustí, S. Accumulation of 13C-labelled phenanthrene in phytoplankton and transfer to corals resolved using cavity ring-down spectroscopy. *Ecotoxicol. Environ. Saf.* **2020**, *196*, No. 110511.
(10) Turner, N. R.; Renegar, D. A. Petroleum hydrocarbon toxicity to corals: a review. *Mar. Pollut. Bull.* **2017**, *119*, 1−16.
(11) Wang, M.; Wang, H.; Zhang, R.; Ma, M.; Mei, K.; Fang, F.; Wang, X. Photolysis of low-brominated diphenyl ethers and their reactive oxygen species-related reaction mechanisms in an aqueous system. *PLoS One* **2015**, *10*, No. e0135400.
(12) Chang, S. S.; Lee, W. J.; Wang, L. C.; Chang-Chien, G. P.; Wu, C. Y. Energy recovery and emissions of PBDD/Fs and PBDEs from cocombustion of woodchip and wastewater sludge in an industrial boiler. *Environ. Sci. Technol.* **2013**, *47*, 12600−12606.
(13) Gobas, F. A. P. C.; Mackintosh, C. E.; Webster, G.; Ikonomou, M.; Parkerton, T. F.; Robillard, K. Bioaccumulation of phthalate esters in aquatic food-webs. In *The Handbook of Environmental Chemistry: Phthalate Esters*; Staples, C. A., Ed.; Springer-Verlag Berlin Heidelberg, V. 3. Part Q, 2003; pp 201−225.
(14) Arfaeinia, H.; Fazlzadeh, M.; Taghizadeh, F.; Saeedi, R.; Spitz, J.; Dobaradaran, S. Phthalate acid esters (PAEs) accumulation in coastal sediments from regions with different land use configuration along the Persian Gulf. *Ecotoxicol. Environ. Saf.* **2019**, *169*, 496−506.
(15) Hankins, C.; Allyn, D.; Kathryn, D. Scleractinian coral microplastic ingestion: potential calcification effects, size limits, and retention. *Mar. Pollut. Bull.* **2018**, *135*, 587−593.
(16) Eriksen, M.; Lebreton, L. C.; Carson, H. S.; Thiel, M.; Moore, C. J.; Borerro, J. C.; Galgani, F.; Ryan, P. G.; Reisser, J. Plastic pollution in the world oceans: more than 5 trillion plastic pieces weighing over 250,000 tons afloat at sea. *PLoS One* **2014**, *9*, No. e111913.
(17) Clark, J. R.; Cole, M.; Lindeque, P. K.; Fileman, E.; Blackford, J.; Lewis, C.; Lenton, T. M.; Galloway, T. G. Marine microplastic debris: a targeted plan for understanding and quantifying interactions with marine life. *Front. Ecol. Environ.* **2016**, *14*, 317−324.
(18) Lohmann, R.; Muir, D.; Zeng, E. Y.; Bao, L. J.; Allan, I. J.; Arinaitwe, K.; Booij, K.; Helm, P.; Kaserzon, S.; Mueller, J. F.; Shibata, Y.; Smedes, F.; Tsapakis, M.; Wong, C. S.; You, J. Aquatic Global Passive Sampling (AQUA-GAPS) revisited: First steps toward a network of networks for monitoring organic contaminants in the aquatic environment. *Environ. Sci. Technol.* **2017**, *51*, 1060−1067.
(19) Shao, M.; Tao, P.; Wang, M.; Jia, H.; Li, Y. F. Trophic magnification of polybrominated diphenyl ethers in the marine food web from coastal area of Bohai Bay, North China. *Environ. Pollut.* **2016**, *213*, 379−385.
(20) Aminot, Y.; Lanctôt, C.; Bednarz, V.; Robson, W. J.; Taylor, A.; Ferrier-Pagès, C.; Metian, M.; Tolosa, I. Leaching of flame-retardants from polystyrene debris: Bioaccumulation and potential effects on coral. *Mar. Pollut. Bull.* **2020**, *151*, No. 110862.
(21) Bekele, T. G.; Zhao, H.; Wang, Q.; Chen, J. Bioaccumulation and trophic transfer of emerging organophosphate flame retardants in the marine food webs of Laizhou Bay, north China. *Environ. Sci. Technol.* **2019**, *53*, 13417−13426.
(22) Jamieson, A. J.; Malkocs, T.; Piertney, S. B.; Fujii, T.; Zhang, Z. Bioaccumulation of persistent organic pollutants in the deepest ocean fauna. *Nat. Ecol. Evol.* **2017**, *1*, No. 0051.
(23) Akhbarizadeh, R.; Moore, F.; Keshavarzi, B.; Moeinpour, A. Microplastics and potentially toxic elements in coastal sediments of Iran's main oil terminal (Khark Island). *Environ. Pollut.* **2017**, *220*, 720−731.
(24) Shuail, D.; Wiedenmann, J.; D'Angelo, C. H.; Baird, A. H.; Pratchett, M. S.; Riegl, B.; Burt, J. A.; Petrov, P.; Amos, C. Local bleaching thresholds established by remote sensing techniques vary among reefs with deviating bleaching patterns during the 2012 event in the Arabian/Persian Gulf. *Mar. Pollut. Bull.* **2016**, *105*, 654−659.
(25) Monroe, A. A.; Ziegler, M.; Anna Roik, A.; Röthig, T.; Hardenstine, R. S.; Emms, M. A.; Jensen, T.; Voolstra, C. R.; Berumen, M. L. In situ observations of coral bleaching in the central Saudi Arabian Red Sea during the 2015/2016 global coral bleaching event. *PLoS One* **2018**, *13*, No. e0195814.
(26) Mohammadizadeh, M.; Tavakoli-Kolour, P.; Rezai, H. Coral reefs and community around larak island (Persian Gulf). *Caspian J. Appl. Sci. Res.* **2013**, *2*, 52−60.
(27) Gilbert, S. F.; Bosch, T. C. G.; Ledón-Rettig, C. Eco-Evo-Devo: developmental symbiosis and developmental plasticity as evolutionary agents. *Nat. Rev. Genet.* **2015**, *16*, 611−622.
(28) WMO. *Report on the WMO-WHO meeting of expert on standardization of UV indices and their dissemination to the public*; World Meteorological Organization: Les Diablerets, Switzerland, Volume *127*, 1998.
(29) WHO. World Meteorological Organization. United Nations Environment Programme & International Commission on Non-Ionizing Radiation Protection. In *Global Solar UV Index: A Practical Guide*; World Health Organization: Geneva, Switzerland, 2002.
(30) Roshan, D. R.; Koc, M.; Abdallah, A.; Martin-Pomares, L.; Isaifan, R.; Fountoukis, C. UV Index forecasting under the influence of desert dust: Evaluation against surface and satellite-retrieved data. *Atmosphere* **2020**, *11*, 96.
(31) APHA, *Standard Methods for the Examination of Water and Wastewater*, 21st ed. American Public Health Association: Washington DC 2005.
(32) Zhang, S.; Bursian, S. J.; Martin, P. A.; Chan, H. M.; Tomy, G.; Palace, V. P.; Mayne, G. J.; Martin, J. W. Reproductive and developmental toxicity of a pentabrominated diphenyl ether mixture, DE-71, to ranch mink (*Mustela vison*) and hazard assessment for wild mink in the Great Lakes region. *Toxicol. Sci.* **2009**, *110*, 107−116.
(33) Wang, J. X.; Lin, Z. K.; Lin, K. F.; Wang, C. Y.; Zhang, W.; Cui, C. Y.; Lin, J. D.; Dong, Q. X.; Huang, C. J. Polybrominated diphenyl ethers in water, sediment, soil, and biological samples from different industrial areas in Zhejiang, China. *J. Hazard. Mater.* **2011**, *197*, 211−219.
(34) Ju, T.; Ge, W.; Jiang, T.; Chai, C. Polybrominated diphenyl ethers in dissolved and suspended phases of seawater and in surface sediment from Jiaozhou Bay, North China. *Sci. Total Environ.* **2016**, *557*−*558*, 571−578.
(35) Saliu, F.; Montano, S.; Leoni, B.; Lasagni, M.; Galli, P. Microplastics as a threat to coral reef environments: Detection of phthalate esters in neuston and scleractinian corals from the Faafu Atoll, Maldives. *Mar. Pollut. Bull* **2019**, *142*, 234−241.
(36) Folch, J.; Lees, M.; Sloane-Stanley, G. A simple method for the isolation and purification of total lipides from animal tissues. *J. Biol. Chem.* **1957**, *226*, 497−509.
(37) Ranjbar Jafarabadi, A.; Riyahi Bakhtiari, A.; Aliabadian, M.; Laetitia, H.; Shadmehri Toosi, A.; Yap, C. K. First report of bioaccumulation and bioconcentration of aliphatic hydrocarbons (AHs) and persistent organic pollutants (PAHs, PCBs and PCNs) and their effects on alcyonacea and scleractinian corals and their endosymbiotic algae from the Persian Gulf, Iran: Inter and intra-species differences. *Sci. Total Environ.* **2018**, *627*, 141−157.
(38) Qiu, Y. W.; Zeng, E. Y.; Qiu, H.; Yu, K.; Cai, S. Bioconcentration of polybrominated diphenyl ethers and organochlorine pesticides in algae is an important contaminant route to higher trophic levels. *Sci. Total Environ.* **2017**, *579*, 1885−1893.
(39) Tuikka, A.; Leppänen, M.; Akkanen, J.; Sormunen, A.; Leonards, P.; van Hattum, B.; van Vliet, L.; Brack, W.; Smedes, F.;

https://doi.org/10.1021/acs.est.0c08730
Environ. Sci. Technol. XXXX, XXX, XXX−XXX

Kukkonen, J. Predicting the bioaccumulation of polyaromatic hydrocarbons and polychlorinated biphenyls in benthic animals in sediments. *Sci. Total Environ.* **2016**, *563*−*564*, 396−404.
(40) Wang, X.; Zhu, L.; Zhong, W.; Yang, L. Partition and source identification of organophosphate esters in the water and sediment of Taihu Lake, China. *J. Hazard. Mater.* **2018**, *360*, 43−50.
(41) Kohonen, T. MATLAB implementations and applications of the Self-Organizing Map. Unigrafia Oy: Helsinki, Finland, 2014, p 201. http://docs.unigrafia.fi/publications/kohonen_teuvo/index.html.
(42) EPA. Environmental Protection Agency. Water Quality Standards − Hand Book − Second edition. EPA − National Guidance Water Quality Standards for Wetlands, August 1994, EPA 823-B-94-005a, 1994; p344.
(43) USEPA. Draft Guidance for Water Quality-Based Decisions: The TMDL Process (Second Edition). (EPA 841-D-99-001). United States Environmental Protection Agency, Office of Water: Washington, D.C., 1999.
(44) Ibrahim, E. H. Nutrient salts, inorganic and organic carbon contents in the waters of the Persian Gulf and the Gulf of Oman. *J. Persian. Gulf* **2010**, *1*, 33−44.
(45) van Dam, J. W.; Negri, A. P.; Uthicke, S.; Mueller, J. F. Chemical pollution on coral reefs: exposure and ecological effects. In *Ecological Impacts of Toxic Chemicals*; Bentham Science Publishers Ltd., 2011; Vol. *9*, pp 187−211.
(46) Riegl, B. M.; Purkis, S. J.; Al-Cibahy, A. S.; Al-Harthi, S.; Grandcourt, E.; Al-Sulaiti, K.; Baldwin, J.; Abdel-Moati, A. M. Coral bleaching and mortality thresholds in the SE Gulf: highest in the world. In *Coral Reefs of the Gulf: Adaptation to Climatic Extremes*; Riegl, B. M.; Purkis, S. J., Eds.; Springer: Berlin, 2012; pp 95−105.
(47) Paparella, F.; Xu, C.; Vaughan, G. O.; Burt, J. A. Coral bleaching in the Persian/Arabian Gulf is modulated by summer winds. *Front. Mar. Sci.* **2019**, *6*, 205.
(48) Ahmad, F.; Sultan, S. A. R. Annual mean surface heat fluxes in the Arabian Gulf and the net heat transport through the Strait of Hormuz. *Atmos.-Ocean* **1991**, *29*, 54−61.
(49) Downs, C. A.; Fauth, J. E.; Halas, J. C.; Dustan, P.; Bemiss, J.; Woodley, C. M. Oxidative stress and seasonal coral bleaching. *Free Radical Biol. Med.* **2002**, *33*, 533−543.
(50) Vaughan, G. O.; Al-Mansoori, N.; Burt, J. The Arabian Gulf. In *World Seas: An Environmental Evaluation*, 2nd ed.; Sheppard, C., Ed.; Elsevier Science: Amsterdam, NL, 2019; pp 1−23.
(51) Riegl, B. Effects of the 1996 and 1998 SST anomalies on corals, coral diseases and fish in the Arabian Gulf (Dubai, UAE). *Mar. Biol.* **2002**, *140*, 29−40.
(52) Riegl, B.; Purkis, S. Coral population dynamics across consecutive mass mortality events. *Global Change Biol.* **2015**, *21*, 3995−4005.
(53) Kavousi, J.; Tavakoli-Kolour, P.; Mohammadizadeh, M.; Bahrami, A.; Barkhordari, A. Mass coral bleaching in the northern Persian Gulf, 2012. *Sci. Mar.* **2014**, *78*, 397−404.
(54) Voolstra, C. R.; Buitrago-López, C.; Perna, G.; Cárdenas, A.; Hume, B. C. C.; Rädecker, N.; Barshis, D. J. Standardized short-term acute heat stress assays resolve historical differences in coral thermotolerance across microhabitat reef sites. *Global Change Biol.* **2020**, *26*, 4328−4343.
(55) Tarrant, A. M.; Reitzel, A. M.; Kwok, C. K.; Jenny, M. J. Activation of the cnidarian oxidative stress response by ultraviolet radiation, polycyclic aromatic hydrocarbons and crude oil. *J. Exp. Biol.* **2014**, *217*, 1444−1453.
(56) Tolleter, D.; Seneca, F. O.; DeNofrio, J. C.; Krediet, C. J.; Palumbi, S. R.; Pringle, J. R.; Grossman, A. R. Coral bleaching independent of photosynthetic activity. *Curr. Biol.* **2013**, *23*, 1782−1786.
(57) Oakley, C. A.; Davy, S. K. Cell biology of coral bleaching. In *Coral Bleaching, Ecological Studies*; van Oppen, M. J. H.; Lough, J. M., Eds.; Springer Int Pub AG, Springer Nature, 2018; p 233.
(58) Burt, J.; Bartholomew, A.; Sale, P. F. Benthic development on large-scale engineered reefs: a comparison of communities among breakwaters of different age and natural reefs. *Ecol. Eng.* **2011**, *37*, 191−198.
(59) Bainbridge, Z.; Lewis, S.; Bartley, R.; Fabricius, K.; Collier, C.; Waterhouse, J.; Garzon-Garcia, A.; Robsonc, B.; Burton, J.; Wenger, A.; Brodie, J. Fine sediment and particulate organic matter: A review and case study on ridge-to-reef transport, transformations, fates, and impacts on marine ecosystems. *Mar. Pollut. Bull.* **2018**, *135*, 1205−1220.
(60) ECA. European Chemicals Agency, Guidance on Information Requirements and Chemical Safety Assessment: Chapter R.11: PBT Assessment (Version 1.1). 2012.
(61) WWF. *Stockholm Convention: "New POPs": screening additional POPs candidates*; World Wildlife Fund: Washington DC, 2005; p 38.
(62) Montano, S.; Seveso, D.; Maggioni, D.; Galli, P.; Corsarini, S.; Saliu, F. Spatial variability of phthalates contamination in the reef-building corals *Porites lutea*, *Pocillopora verrucosa* and *Pavona varians*. *Mar. Pollut. Bull.* **2020**, *155*, No. 111117.
(63) Wan, Y.; Hu, J.; Zhang, K.; An, L. Trophodynamics of polybrominated diphenyl ethers in the marine food web of Bohai Bay, North China. *Environ. Sci. Technol.* **2008**, *42*, 1078−1083.
(64) Guest, J. R.; Low, J.; Tun, K.; Wilson, B.; Ng, C.; Raingeard, D.; Ulstrup, K. E.; Tanzil, J. T. I.; Todd, P. A.; Toh, T. C.; McDougald, D.; Chou, L. M.; Steinberg, P. D. Coral community response to bleaching on a highly disturbed reef. *Sci. Rep.* **2016**, *6*, No. 20717.
(65) Caroselli, E.; Frapiccini, F.; Franzellitti, S.; Palazzo, Q.; Prada, F.; Betti, M.; Goffredo, S.; Marini, M. Accumulation of PAHs in the tissues and algal symbionts of a common Mediterranean coral: Skeletal storage relates to population age structure. *Sci. Total Environ.* **2020**, *743*, No. 140781.
(66) Ko, F. C.; Chang, C. W.; Cheng, J. O. Comparative study of polycyclic aromatic hydrocarbons in coral tissues and the ambient sediments from Kenting National Park, Taiwan. *Environ. Pollut.* **2014**, *185*, 35−43.
(67) Michalek-wagner, K.; Bowden, B. F. Effects of bleaching on secondary metabolite chemistry of alcyonacean soft corals. *J. Chem. Ecol.* **2000**, *26*, 1543−1562.
(68) Slattery, M.; Pankey, M. S.; Lesser, M. P. Annual thermal stress increases a soft coral's susceptibility to bleaching. *Sci. Rep.* **2019**, *9*, No. 8064.
(69) Strychar, K. B.; Coates, T. M.; Sammarco, P. W.; Piva, T. J.; Scott, P. T. Loss of Symbiodinium from bleached soft corals *Sarcophyton ehrenbergi*, *Sinularia sp*. and *Xenia sp*. *J. Exp. Mar. Biol. Ecol.* **2005**, *320*, 159−177.
(70) Imbs, A. B. Fatty acids and other lipids of corals: composition, distribution and biosynthesis. *Russ. J. Mar. Biol.* **2013**, *39*, 153−168.
(71) Salvadó, J. A.; Grimalt, J.; López, J.; de Madron, X. D.; Heussner, S.; Canals, M. Transformation of PBDE mixtures during sediment transport and resuspension in marine environments (Gulf of Lion, NW Mediterranean Sea). *Environ. Pollut.* **2012**, *168*, 87−95.
(72) Lipp, E. K.; Griffin, D. W. Analysis of coral mucus as an improved medium for detection of enteric microbes and for determining patterns of sewage contamination in reef environments. *EcoHealth* **2004**, *1*, 317−323.
(73) Cunha, C.; Paulo, J.; Faria, M.; Kaufmann, M.; Cordeiro, N. Ecotoxicological and biochemical effects of environmental concentrations of the plastic-bond pollutant dibutyl phthalate on Scenedesmus Sp. *Aquat. Toxicol.* **2019**, *215*, No. 105281.
(74) Gardner, S. G.; Camp, E. F.; Smith, D. J.; Kahlke, T.; Osman, E. O.; Gendron, G.; Hume, B. C. C.; Pogoreutz, C.; Voolstra, C. R.; Suggett, D. J. Coral microbiome diversity reflects mass coral bleaching susceptibility during the 2016 El Niño heat wave. *Ecol. Evol.* **2019**, *9*, 938−956.
(75) Sampayo, E. M.; Ridgway, T.; Bongaerts, P.; Hoegh-Guldberg, O. Bleaching susceptibility and mortality of corals are determined by fine-scale differences in symbiont type. *Proc. Natl. Acad. Sci. U.S.A.* **2008**, *105*, 10444−10449.
(76) Chou, L. M.; Toh, T. C.; Toh, K. B.; Ng, C. S. L.; Cabaitan, P.; Tun, K.; Goh, E.; Afiq-Rosli, L.; Taira, T.; Du, R. C. P.; Loke, H. X.; Khalis, A.; Li, J.; Song, T. Differential response of coral assemblages to

https://doi.org/10.1021/acs.est.0c08730
Environ. Sci. Technol. XXXX, XXX, XXX−XXX

thermal stress underscores the complexity in predicting bleaching susceptibility. *PLoS One* **2016**, *11*, No. e0159755.
(77) Guest, J. R. J. R.; Low, J.; Tun, K.; Tanzil, J. I.; Todd, P. A.; Toh, T. C.; Chou, L. M.; Steinberg, P. D. Coral community bleaching response on a highly urbanised reef. Peer. *J. Preprints* **2014**, *2*, No. e760v1.
(78) Zhou, J.; Chen, J.; Liang, C. H.; Xie, Q.; Wang, Y. N.; Zhang, S.; Qiao, X.; Li, X. Quantum chemical investigation on the mechanism and kinetics of PBDE photooxidation by.OH: A case study for BDE-15. *Environ. Sci. Technol.* **2011**, *45*, 4839−4845.
(79) Wild, C.; Huettel, M.; Klueter, A.; Kremb, S. G.; Rasheed, M. Y. M.; Jørgensen, B. B. Coral mucus functions as an energy carrier and particle trap in the reef ecosystem. *Nature* **2004**, *428*, 66−70.
(80) Razzaghi, M.; Mashjoor, S.; Kamrani, E. Mean trophic level of coastal fisheries landings in the Persian Gulf (Hormuzgan Province), 2002−2011. *Chin. J. Oceanol. Limnol.* **2017**, *35*, 528−536.
(81) Aronson, R. B.; Precht, W. F. Conservation, precaution, and Caribbean reefs. *Coral Reefs* **2006**, *25*, 441−450.
(82) Willemsen, J. A. R.; Myneni, S. C. B.; Bourg, I. C. Molecular dynamics simulations of the adsorption of phthalate esters on smectite clay surfaces. *J. Phys. Chem. C* **2019**, *123*, 13624−13636.
(83) Braekevelt, E.; Tittlelier, S. A.; Tomy, G. Direct measurement of octanol-water partition coefficients of some environmentally relevant brominated diphenyl ether congeners. *Chemosphere* **2003**, *51*, 563−567.
(84) Kong, L.; Ferry, J. L. Effect of salinity on the photolysis of chrysene adsorbed to a smectite clay. *Environ. Sci. Technol.* **2003**, *37*, 4894−4900.
(85) Wang, Y.; Wu, X.; Zhao, H.; Xie, Q.; Hou, M.; Zhang, Q.; Du, J.; Chen, J. Characterization of PBDEs and novel brominated flame retardants in seawater near a coastal mariculture area of the Bohai Sea, China. *Sci. Total Environ.* **2017**, *580*, 1446−1452.
(86) Wang, R.; Tang, T.; Wei, Y.; Dang, D.; Huang, K.; Chen, X.; Yin, H.; Tao, X.; Lin, Z.; Dang, Z.; Lu, G. Photocatalytic debromination of polybrominated diphenyl ethers (PBDEs) on metal doped TiO2 nanocomposites: Mechanisms and pathways. *Environ. Int.* **2019**, *127*, 5−12.
(87) Wang, R.; Tang, T.; Xie, J.; Tao, X.; Huang, K.; Zou, M.; Yin, H.; Dang, Z.; Lu, G. Debromination of polybrominated diphenyl ethers (PBDEs) and their conversion to polybrominated dibenzofurans (PBDFs) by UV light: mechanisms and pathways. *J. Hazard. Mater.* **2018**, *354*, 1−7.
(88) Maier, S. R.; Kutti, T.; Bannister, R. J.; Fang, J. K. H.; van Breugel, P.; van Rijswijk, P.; van Oevelen, D. Recycling pathways in cold-water coral reefs: Use of dissolved organic matter and bacteria by key suspension feeding taxa. *Sci. Rep.* **2020**, *10*, No. 9942.
(89) Glasl, B.; Herndl, G. J.; Frade, P. R. The microbiome of coral surface mucus has a key role in mediating holobiont health and survival upon disturbance. *ISME J.* **2016**, *10*, 2280−2292.
(90) Coles, S. L.; Strathmann, R. Observations on coral mucus "flocs" and their potential trophic significance. *Limnol. Oceanogr.* **1973**, *18*, 673−678.
(91) Hadaidi, G.; Gegner, H. M.; Ziegler, M.; Voolstra, C. R. Carbohydrate composition of mucus from scleractinian corals from the central Red Sea. *Coral Reefs* **2019**, *38*, 21−27.
(92) Brown, B.; Bythell, J. Perspectives on mucus secretion in reef corals. *Mar. Ecol. Prog. Ser.* **2005**, *296*, 291−309.
(93) Tian, R. M.; Lee, O. O.; Wang, Y.; Cai, L.; Bougouffa, S.; Chiu, M. Y.; Wu, R. S. S.; Qian, P. Y. Effect of polybrominated diphenyl ether (PBDE) treatment on the composition and function of the bacterial community in the sponge *Haliclona cymaeformis*. *Front. Microbiol.* **2015**, *5*, 799.
(94) Nakajima, R.; Tanaka, Y. The role of coral mucus in the material cycle in reef ecosystems: Biogeochemical and ecological perspectives. *J. Jpn. Coral Reef Soc.* **2014**, *16*, 3−27.
(95) Mengchen, L. V.; Tang, X.; Zhao, Y.; Li, J.; Zhang, B.; Li, L.; Jiang, Y.; Zhao, Y. The toxicity, bioaccumulation and debromination of BDE-47 and BDE-209 in Chlorella sp. under multiple exposure modes. *Sci. Total Environ.* **2020**, *723*, No. 138086.
(96) Shen, C.; Wang, Y.; Shen, Q.; Wang, L.; Lu, Y.; Li, X.; Wei, J. Di-(2-ethylhexyl) phthalate induced the growth inhibition and oxidative damage in the microalga *Chlorella vulgaris*. *IOP Conf. Ser.: Earth Environ. Sci.* **2019**, *227*, No. 052054.
(97) Gu, S.; Zheng, H.; Xu, Q.; Sun, C.; Shi, M.; Wang, Z.; Fengmin, Li. Comparative toxicity of the plasticizer dibutyl phthalate to two freshwater algae. *Aquat. Toxicol.* **2017**, *191*, 122−130.
(98) Köksal, Ç.; Nalbantsoy, A.; Yavaşoğlu, N. U. K. Cytotoxicity and genotoxicity of butyl cyclohexyl phthalate. *Cytotechnology* **2016**, *68*, 213−222.
(99) Douglas, G. R.; Hugenholtz, A. P.; Blakey, D. H. Genetic toxicology of phthalate esters: mutagenic and other genotoxic effects. *Environ. Health Perspect.* **1986**, *65*, 255−262.
(100) Slattery, M.; Paul, V. I. Indirect effects of bleaching on predator deterrence in the tropical Pacific soft coral *Sinularia maxima*. *Mar. Ecol. Prog. Ser.* **2008**, *354*, 169−179.
(101) Shick, J. M. The continuity and intensity of ultraviolet irradiation affect the kinetics of biosynthesis, accumulation, and conversion of mycosporine-like amino acids (MAAs) in the coral *Stylophora pistillata*. *Limnol. Oceanogr.* **2004**, *49*, 442−458.
(102) Chiwetalu, U. J.; Mbajiorgu, C. C.; Ogbuagu, N. J. Remedial ability of maize (zea-mays) on lead contamination under potted condition and non-potted field soil condition[J]. *J. Bioresour. Bioprod.* **2020**, *5*, 51−59.
(103) Zaimes, G. N.; Tsioras, P. A.; Kiosses, C.; et al. Perspectives on protected area and wildfire management in the Black Sea region[J]. *J. For. Res.* **2020**, *31*, 257−268.

https://doi.org/10.1021/acs.est.0c08730
Environ. Sci. Technol. XXXX, XXX, XXX−XXX